

Proton-proton bremsstrahlung calculations at 280 MeV

V. R. Brown and P. L. Anthony

Lawrence Livermore National Laboratory, P.O. Box 808, Livermore, California 94550

J. Franklin

Physics Department, Temple University, Philadelphia, Pennsylvania 19122

(Received 22 April 1991)

Proton-proton bremsstrahlung calculations are compared to the 280-MeV experimental results from TRIUMF, which use a polarized proton beam. Calculations are included for all experimental results. The Bonn radial potential is compared to a modified Hamada-Johnston and the Bryan-Gersten potentials. Potentials with different short-range radial behavior are compared in order to examine the penetration of the photon radiation. Rather good agreement with experiment for the Bonn potential is achieved without the arbitrary normalization of $\frac{2}{3}$ applied to the TRIUMF cross-section data. The rescattering included in our work accounts for an increase of up to approximately 20% in the cross section, which is not large enough to explain the differences with other calculations, and it contributes up to a factor of 2.5 in the analyzing power. Our present results include partial waves up to $J_{\max} = 6$.

I. INTRODUCTION

Nucleon-nucleon bremsstrahlung, $NN\gamma$, is a fundamental process, which involves the strong and electromagnetic (EM) fields acting simultaneously. Since the electromagnetic interaction is well known, $NN\gamma$ provides a calculable tool for comparing off-energy-shell effects from different two-nucleon potentials compared to experiment and also provides a simple testing ground which is sensitive to meson-exchange-current contributions that are so important in electronuclear physics. Historically, experimental studies have focused on $pp\gamma$, with only a few measurements of $np\gamma$. Interest in $np\gamma$ has recently blossomed because of the role it plays in heavy-ion reactions. Analyzing-power measurements and γ angular distribution measurements at TRIUMF, suggesting a high degree of sensitivity to off-shell effects, are responsible for renewed interest in $pp\gamma$. In addition, a new experimental facility, COSY, under construction at Jülich, Germany, has been designed to improve the experimental accuracy, cover a larger phase space, and better access the maximum off-shell behavior in $pp\gamma$.

$NN\gamma$ comes in three varieties: $np\gamma$, $pp\gamma$, and $nn\gamma$. $pp\gamma$ has been studied most extensively, primarily for investigating the off-energy-shell behavior of the two-nucleon (NN) interaction. In an early paper [1] it was proposed to study small nucleon exit angles (e.g., in the Harvard geometry), higher energies, and polarization to reveal more of the off-shell behavior. The use of relativistic kinematics and the use of the covariant (Moller) form for calculating $NN\gamma$ cross sections, used in Ref. [1], is still used today. That paper [1] presented results for a wide range of kinematics, including 200 and 300 MeV with nucleon exit angles of 10° and 20° in the Harvard geometry comparing a meson-exchange [2] and a hard-core [3] potential. Recent $pp\gamma$ experiments [4,5] at TRIUMF are now examining this kinematical region. The results correspond to our early calculations but for

slightly different kinematics.

Differential-cross-section calculations [4] using the Bonn [6] and Paris [7] potentials were considerably smaller than the TRIUMF data. As stated in Ref. [4], the experimental cross sections in Table I and the corresponding figures of Ref. [4] were multiplied by a factor of $\frac{2}{3}$ to facilitate the comparison with their theoretical cross sections. In this paper we present calculations for the specific cross sections and asymmetries measured in the latest [4] TRIUMF work and find reasonable agreement with their experimental cross sections without the factor of $\frac{2}{3}$.

The calculations are done in the same way as described in Ref. [1]. Our codes have been expanded to include partial waves up to $J_{\max} = 6$. The $NN\gamma$ T -matrix diagrams, treating the nuclear interaction exactly and the electromagnetic interaction to first order, are shown in Fig. 1. The first four diagrams, where the photon is emitted from an external proton leg of the diagram, are often called the pole terms. The last two T -matrix diagrams are called the rescattering or double scattering contribution; these terms, which involve the photon emission occurring between successive nuclear scatterings, start out one order higher in the photon momentum.

In the present paper, the Bonn radial potential [6,8] is compared to the Bryan-Gersten [9] (fit D) and the modified Hamada-Johnston [3,10] potentials. The Hamada-Johnston potential is modified to eliminate the unwanted bound state that occurred for triplet-even waves at high energy in the original potential. Even though the Bryan-Gersten and Hamada-Johnston potentials are fitted to older data sets, they are included because it is important to compare potentials with different short-range radial behavior as a measure of the penetration of the photon radiation. The Bryan-Gersten potential is interesting to compare because it has the effect of meson widths included and a different tensor force than the Bonn potential. We have shown the importance of

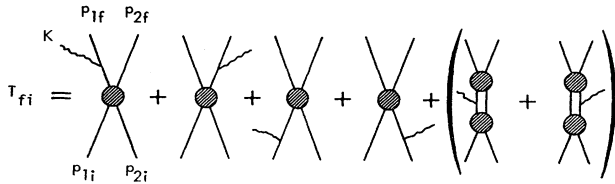


FIG. 1. The T -matrix diagrams for $pp\gamma$ to first order in the electromagnetic interaction including rescattering. The circle with shaded lines represents the nuclear interaction, which is treated exactly with the various NN potentials. The first four diagrams, where the photons are emitted from external legs, are called the pole terms; the last two diagrams in parentheses are the rescattering or double-scattering contributions.

the tensor contribution to $pp\gamma$ in our earlier work [1].

As yet, there is no two-nucleon interaction based on a theory of strong interactions, such as QCD. Meanwhile, boson-exchange potentials fitted to data serve as the “fundamental” or “realistic” interaction operational in nuclear physics. One-boson-exchange potentials, such as the Bryan-Scott [2] potential, are taken from field theory and are represented by Feynman diagrams for the various mesons included in the parametrization. The Bryan-Scott potential is a momentum-dependent one-boson-exchange potential characterized by the exchange of three isoscalar and three isovector mesons; each set of three includes a vector, a pseudoscalar, and a scalar meson, fitted to S and higher partial waves utilizing a linear Feynman cutoff parameter. The nonrelativistically-reduced potential is defined such that when it is inserted into the Schrödinger equation, it yields in Born approximation the same scattering matrix element as the Feynman diagram for one-boson exchange. More modern potentials are similarly defined, but have additional explicit contributions such as meson-width effects, two-pion exchange, and contributions from delta degrees of freedom.

In examining the off-energy-shell behavior, it is important to perform experiments that maximize the off-energy-shell behavior of the nuclear interaction being examined in order to probe the short-range interaction, which is not unambiguously determined by elastic scattering. For $NN\gamma$ this means going beyond the long-wavelength limit of the EM interaction, which sees primarily the long-range pion tail, which is common to most potentials. One needs to examine potentials sufficiently far off shell to see differences that are due to the short-range behavior. The TRIUMF experiment was designed to investigate more of the off-shell contributions to $NN\gamma$ than had been measured previously. A soft-photon calculation [4,11], was used to determine the amount of off-energy-shell information.

II. RESULTS

The TRIUMF geometry shown in Fig. 2 is the Harvard geometry, in which the final protons are observed in coincidence, at unequal angles to, and in the same plane

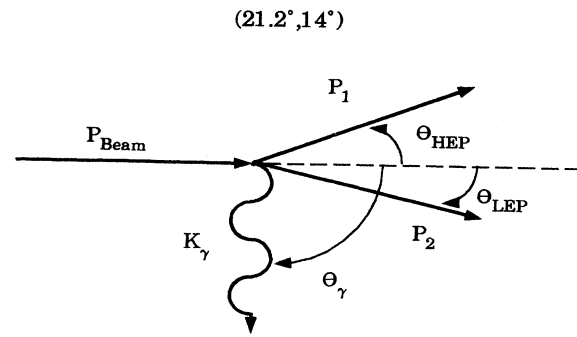


FIG. 2. Kinematics of the TRIUMF (Harvard) geometry, in which the final protons are observed in coincidence, at unequal angles to, and in the same plane as, the incident beam, thereby restricting the photon to this plane as well. The outgoing higher-energy proton (HEP) side of the beam is labeled as particle 1. The photon is observed on the lower-energy proton (LEP) side of the beam from 0° to 180° . The proton angles in parentheses follow the convention throughout the figures that the first (second) one is the HEP (LEP) angle.

as, the incident beam, thereby restricting the photon to this plane as well. The outgoing higher-energy proton (HEP) side of the beam is labeled as particle 1. The photon is observed on the lower-energy proton (LEP) side of the beam from 0° to 180° . The proton angles in parentheses follow the convention throughout this paper that the first (second) one is the HEP (LEP) angle. The HEP and LEP labels are in the convention of Ref. [4] and pertain to how the protons were detected. It should be noted that there are circumstances, e.g. when the HEP angle is larger than the LEP angle, in which the LEP proton can have a higher energy than the HEP proton.

The differential cross sections $d^3\sigma/d\Omega_1 d\Omega_2 d\theta_\gamma$ corresponding to the photon angular distribution for fixed proton coplanar angles in the Harvard geometry are shown [12] for the Bonn radial potential (Bonn) compared to the Bryan-Gersten (BG) and the modified Hamada-Johnston (HJ) potentials in comparison to the TRIUMF data in Figs. 3–8. The label “total” corresponds to the inclusion of all diagrams in Fig. 1. The data as plotted here are from Table II of Ref. [4] with the arbitrary scaling factor of $\frac{2}{3}$ removed. The data include HEP angles of 12.4° , 17.3° , 21.2° , and 27.8° ; each HEP angle includes the LEP angles 12° , 16° , 20° , 24° , and 28° .

In order to illustrate certain features of the calculation, Fig. 9 shows the differential cross section and analyzing power for 280 MeV ($40^\circ, 40^\circ$), which is close to the elastic-scattering geometry.

Figures 10–13 show the photon angular distribution of the analyzing power A_y for the three potentials compared to data. The convention is that the scattering plane is the x - z plane. The data as plotted here are from Table I of Ref. [4]. The data include HEP angles of 12.4° , 17.3° , 21.2° , and 27.8° ; each HEP angle includes the LEP angles 14° , 22° , and 28° .

Figures 7 and 12 show the effect of rescattering. The curves labeled “pole” are calculated from the first four

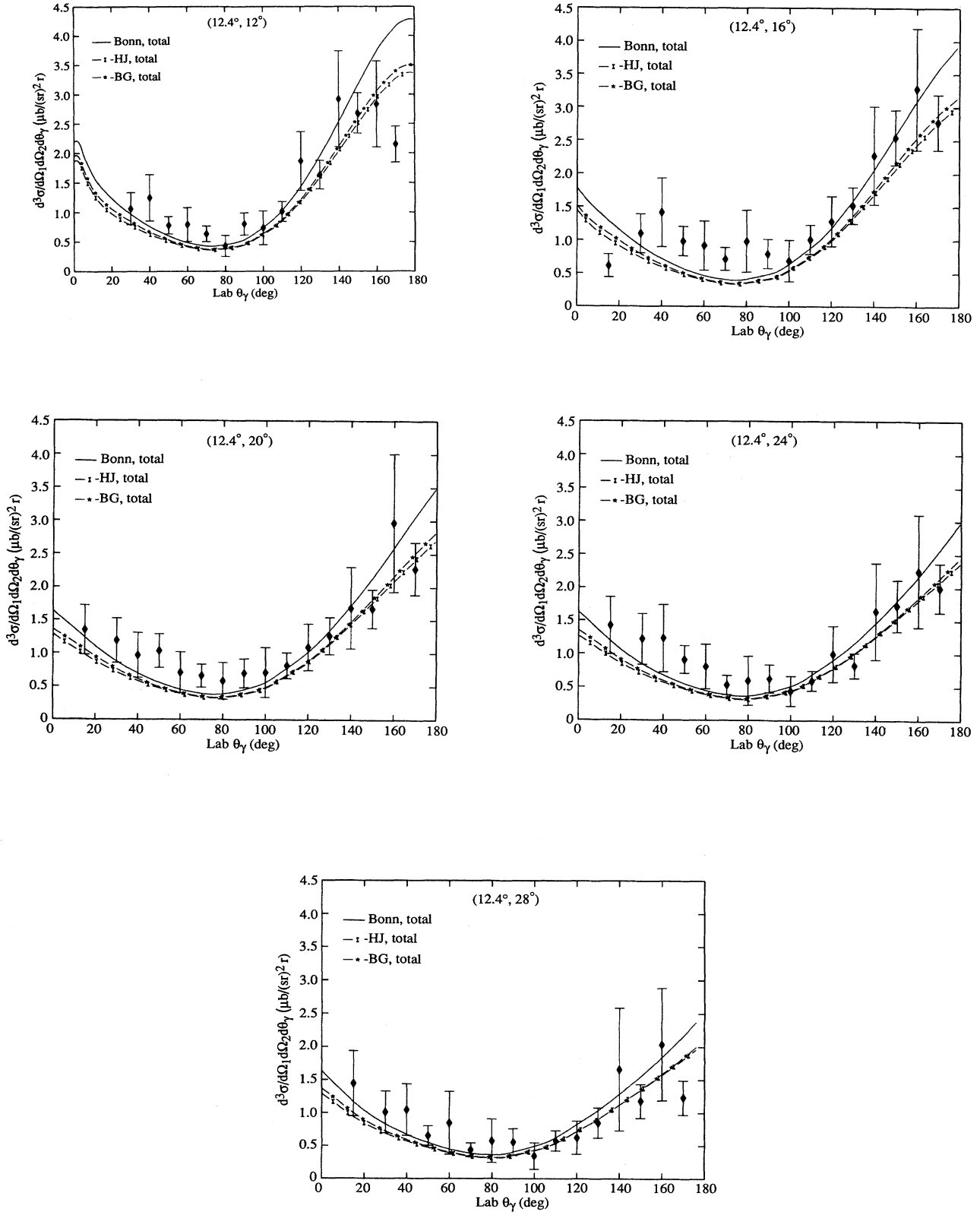


FIG. 3. The coplanar $pp\gamma$ differential cross sections $d^3\sigma/d\Omega_1 d\Omega_2 d\theta_\gamma$ shown for the radial Bonn (Bonn), the Bryan-Gersten (BG), and the modified Hamada-Johnston (HJ) potentials in comparison to the TRIUMF data at 280 MeV. The results are shown for the high-energy proton (HEP) fixed angle of 12.4° and the low-energy proton (LEP) angles 12° , 16° , 20° , 24° , and 28° . See the text and Fig. 2.

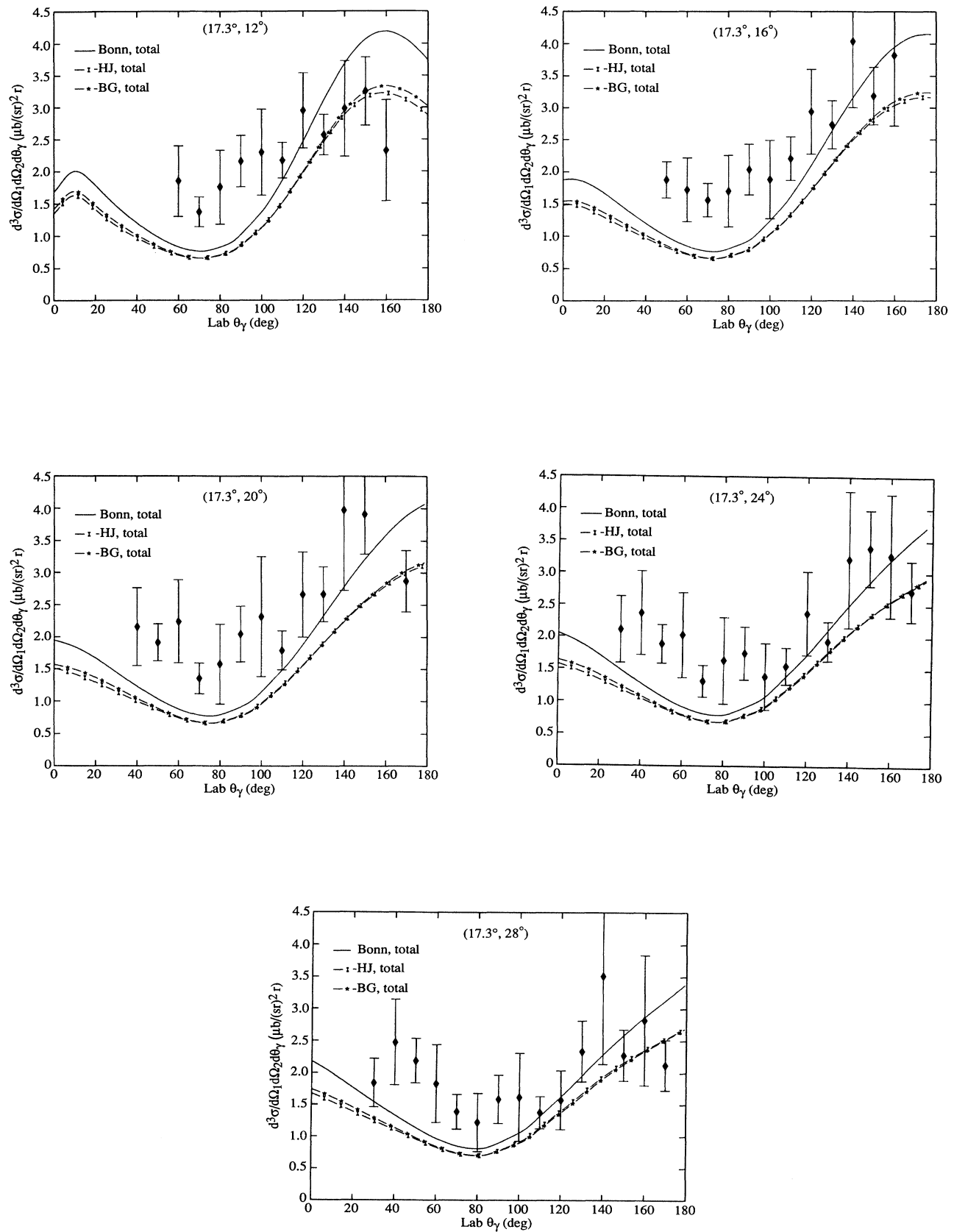
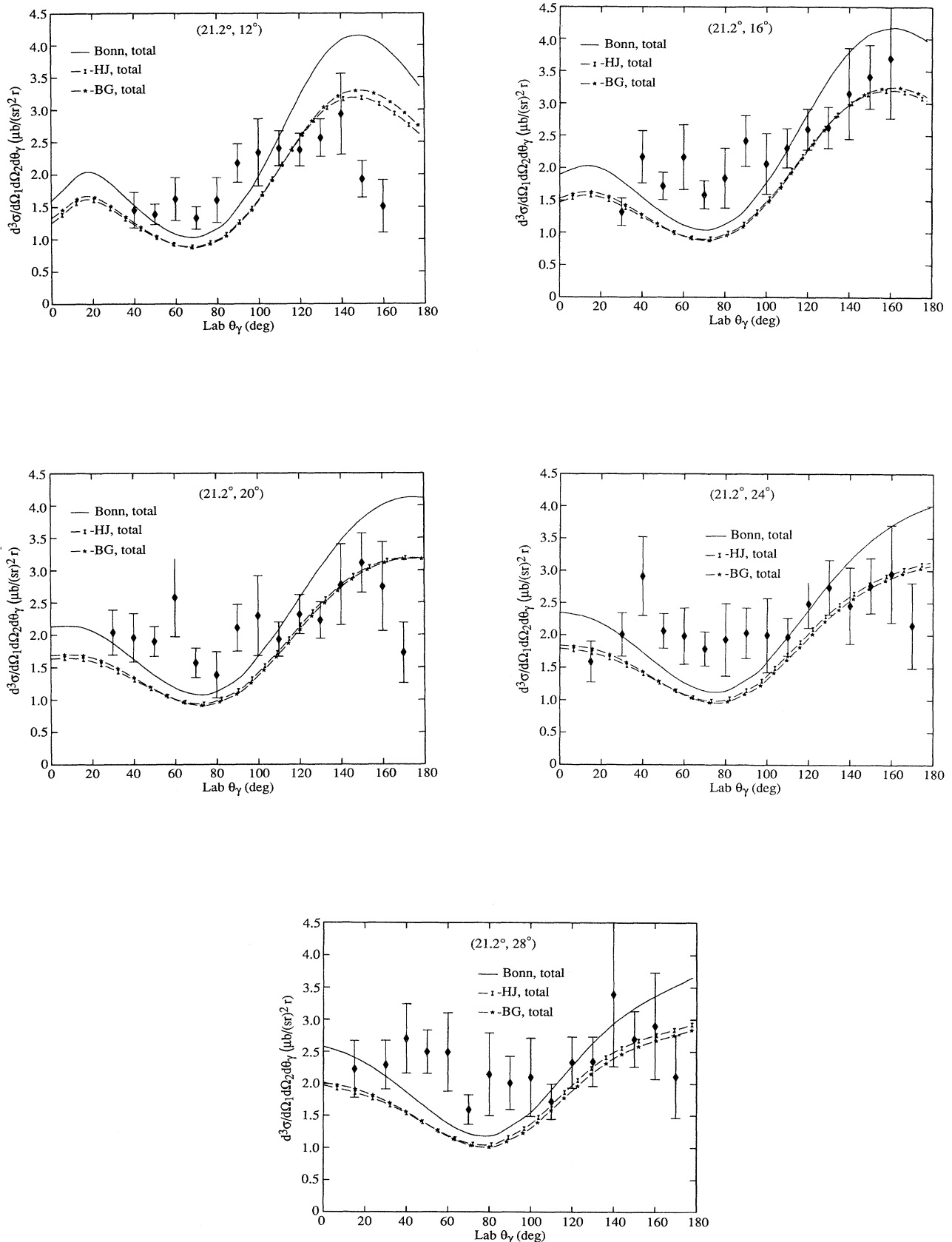


FIG. 4. The same as Fig. 3 for a HEP angle of 17.3° .

FIG. 5. The same as Fig. 3 for a HEP angle of 21.2° .

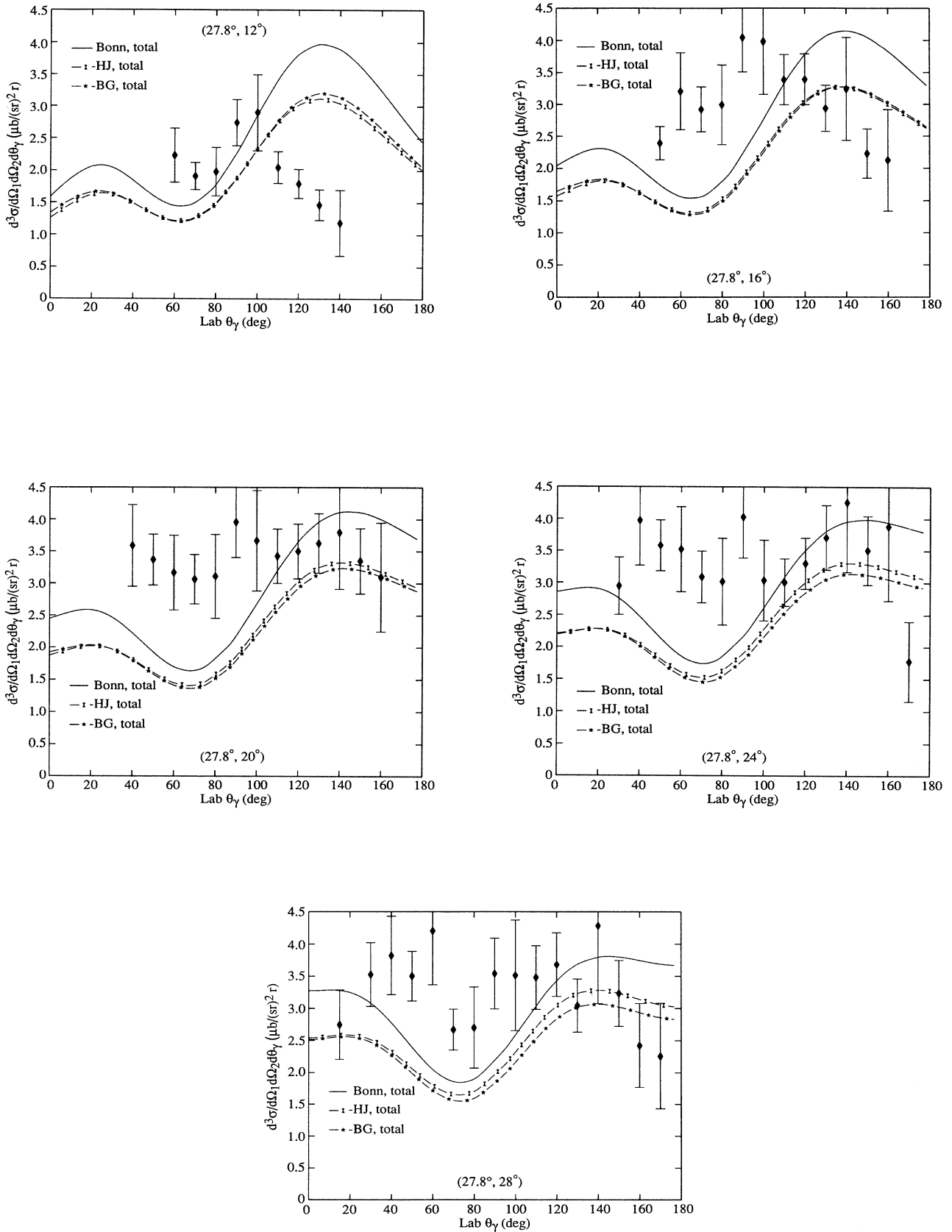


FIG. 6. The same as Fig. 3 for a HEP angle of 27.8° .

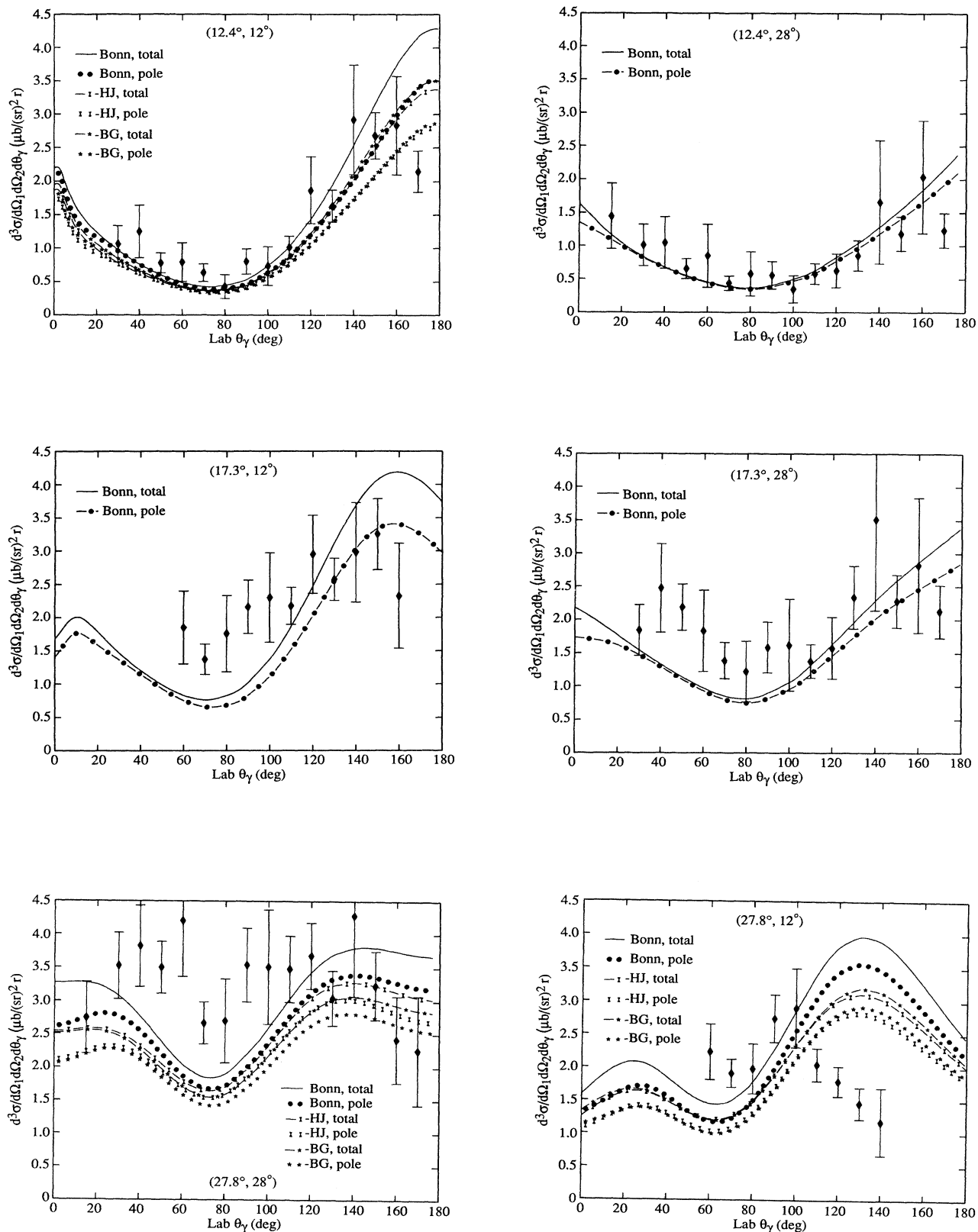


FIG. 7. The same as Fig. 3 with the contribution from the four-pole diagrams (pole) shown separately from that for all six T -matrix diagrams (total), which include the rescattering. The geometries shown are representative samples from Figs. 3, 4, and 6. The Bonn potential is shown alone in three cases for ease in reading.

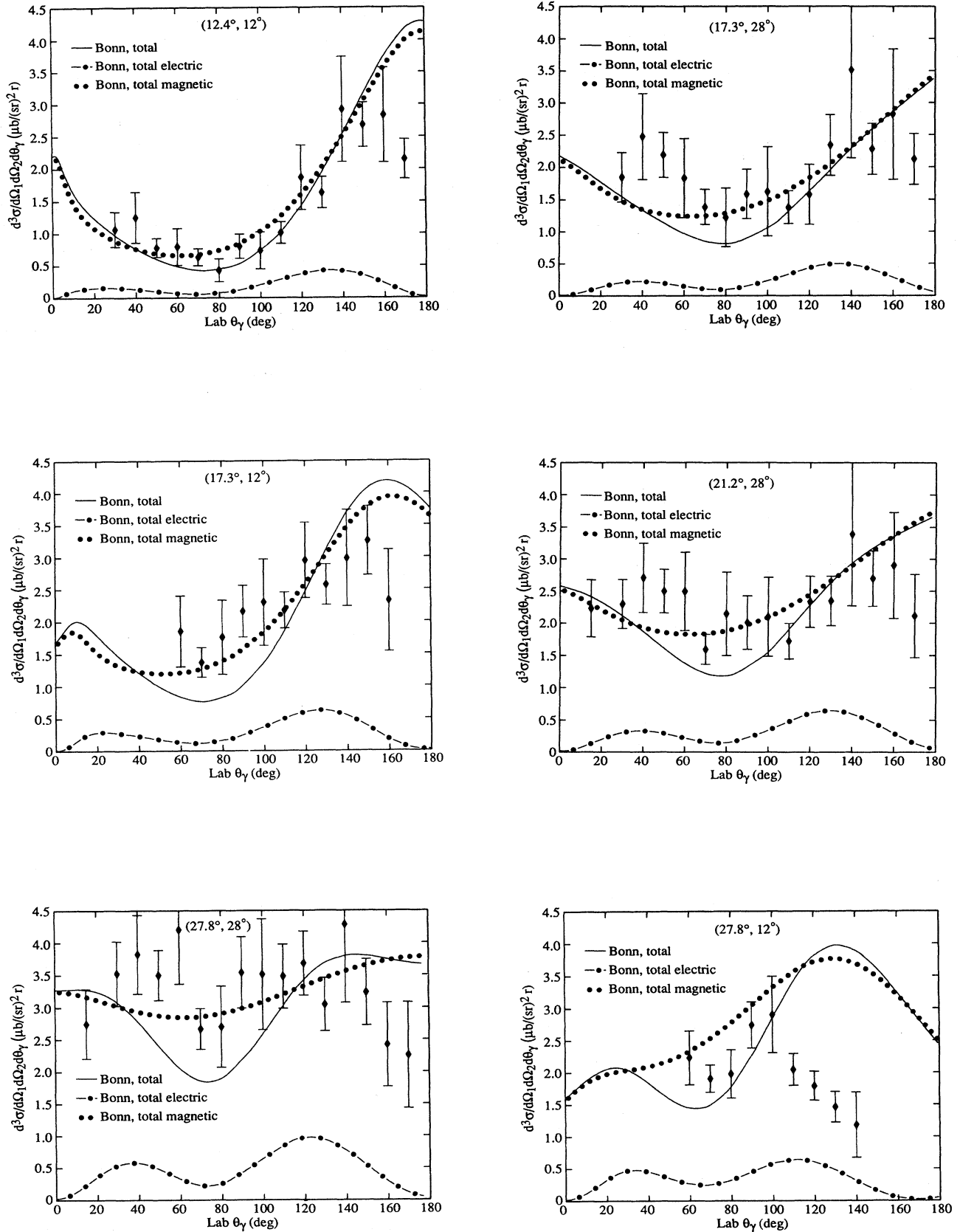


FIG. 8. The same as Fig. 7 with the electric and magnetic contributions to the total cross section separated (see text).

diagrams of Fig. 1. The “total” calculation includes the rescattering, and it corresponds to evaluating all six T -matrix diagrams of Fig. 1. As can be seen in Fig. 7, the rescattering contribution increases the differential cross section typically up to 20%. As can be seen in Fig. 12, depending on θ_γ , the rescattering can increase the magnitude of A_y up to a factor of approximately 2.5. The inclusion of rescattering changes the angular distribution of the analyzing power in a similar way for the three potentials.

The analyzing power is the ratio of the difference over the sum of the cross sections for the beam polarized up and down with respect to the scattering plane. Since the absolute values of the cross sections go out in this ratio, the comparison to the calculations and data of Ref. [4] no longer involves the arbitrary scaling factor of $\frac{2}{3}$. As can be seen in Figs. 10 and 11, the present analyzing-power calculations [13] tend to be larger in magnitude than the calculations in Ref. [4]. As can be seen in Fig. 12, this is

due, primarily, to the magnetic rescattering, which can be large and which is not included in their [4] calculation. One also expects differences due to the different potentials used in Ref. [4] as well as the inclusion of relativistic-spin corrections in that calculation.

Since for $pp\gamma$ the charge-to-mass ratio is the same for each nucleon, the leading electric multipole is not dipole ($E1$) but quadrupole ($E2$) for the photon angular distribution. A not so well known result is that the leading contribution to the photon angular distribution, at least for smaller (in the direction away from the elastic limit) nucleon exit angles in the Harvard geometry, is dominated by the magnetic dipole ($M1$), coming from the coupling of the magnetic moments of the protons to the electromagnetic field. This effect is clearly demonstrated in Figs. 8 and 13, where the electric and magnetic contributions to the differential cross section are separated.

As the sum of the nucleon exit angles (in the Harvard geometry) increases to the near elastic (nonrelativistic

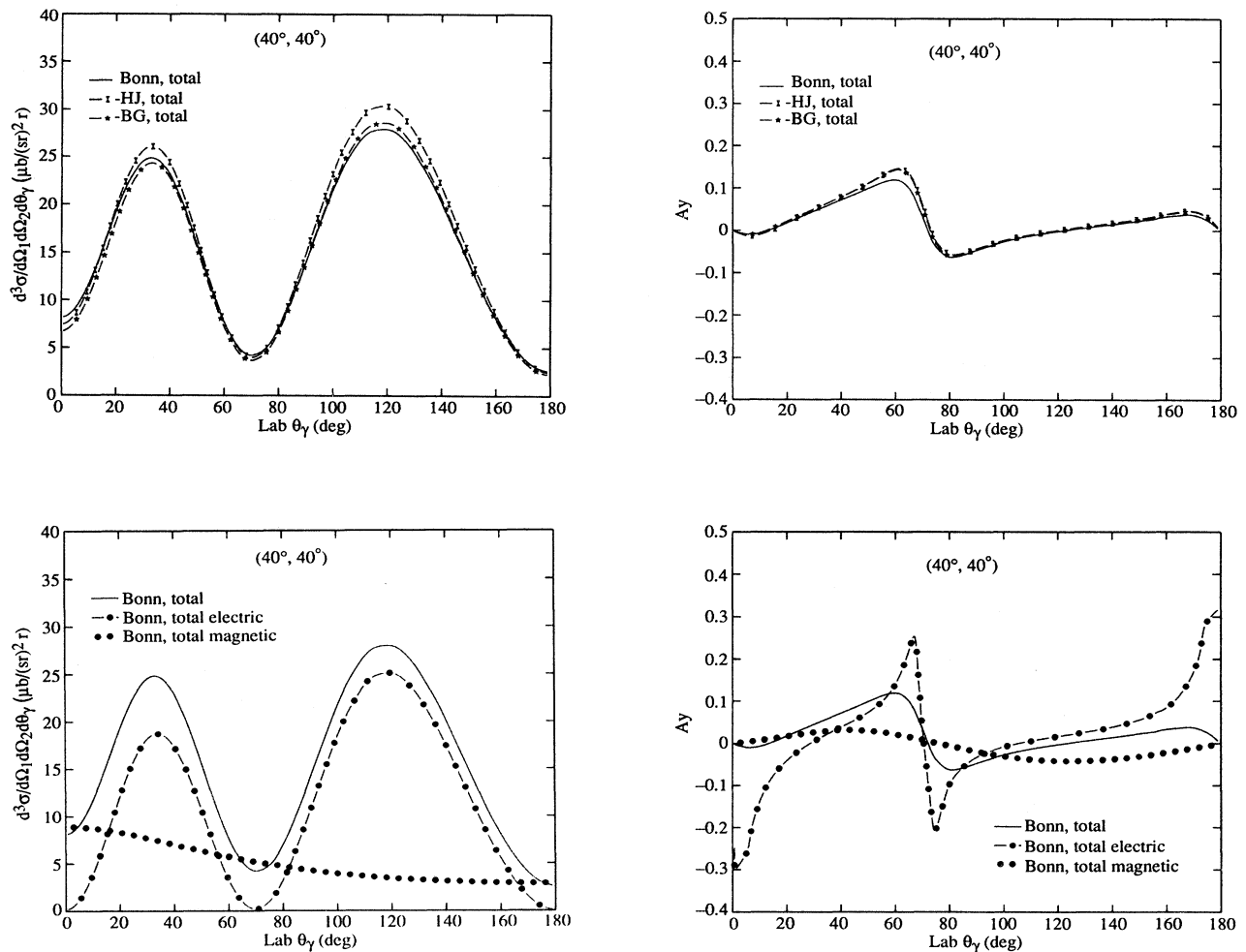


FIG. 9. The coplanar $pp\gamma$ differential cross sections $d^3\sigma/d\Omega_1d\Omega_2d\theta_\gamma$ and the analyzing power A_y calculated for the three potentials at 280 MeV with equal proton exit angles of 40° . The total electric and magnetic contributions are separated and compared for the Bonn potential.

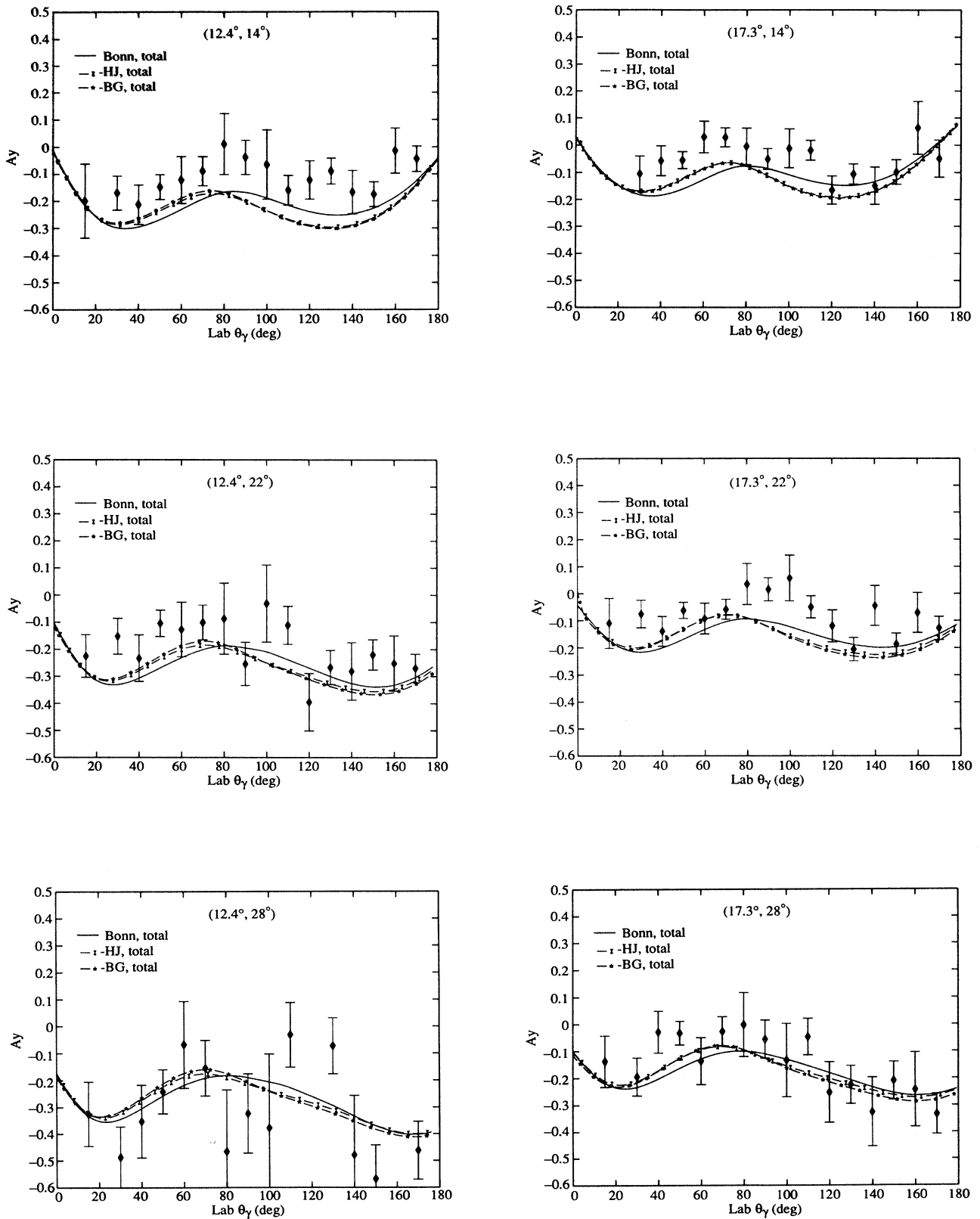


FIG. 10. The analyzing power A_y is shown for the radial Bonn (Bonn), the Bryan-Gersten (BG), and the modified Hamada-Johnston (HJ) potentials in comparison to the TRIUMF data at 280 MeV. The results are shown for HEP angles of 12.4° and 17.3°; each HEP angle includes the LEP angles 14°, 22°, and 28°.

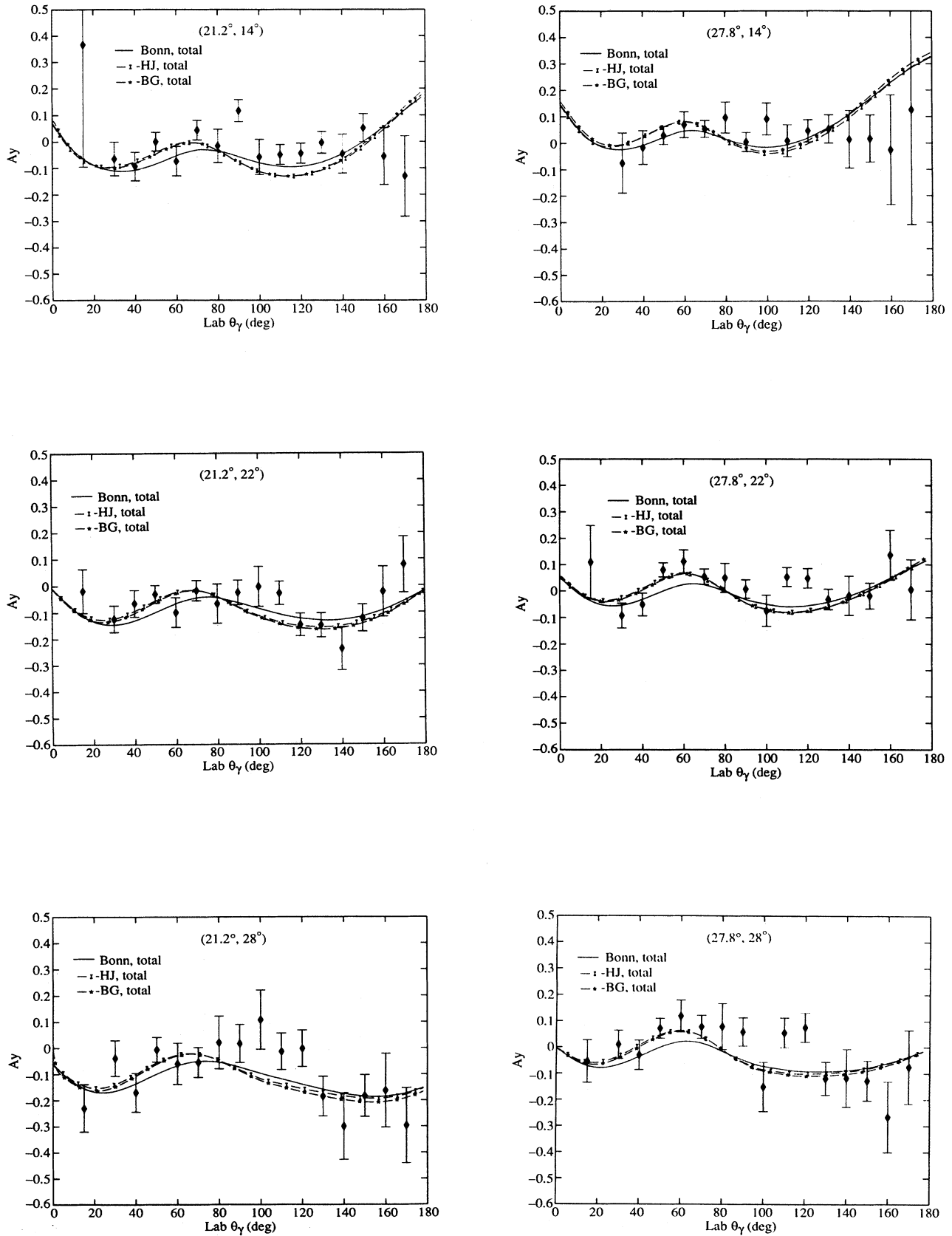


FIG. 11. The same as Fig. 11 for HEP angles of 21.2° and 27.8° .

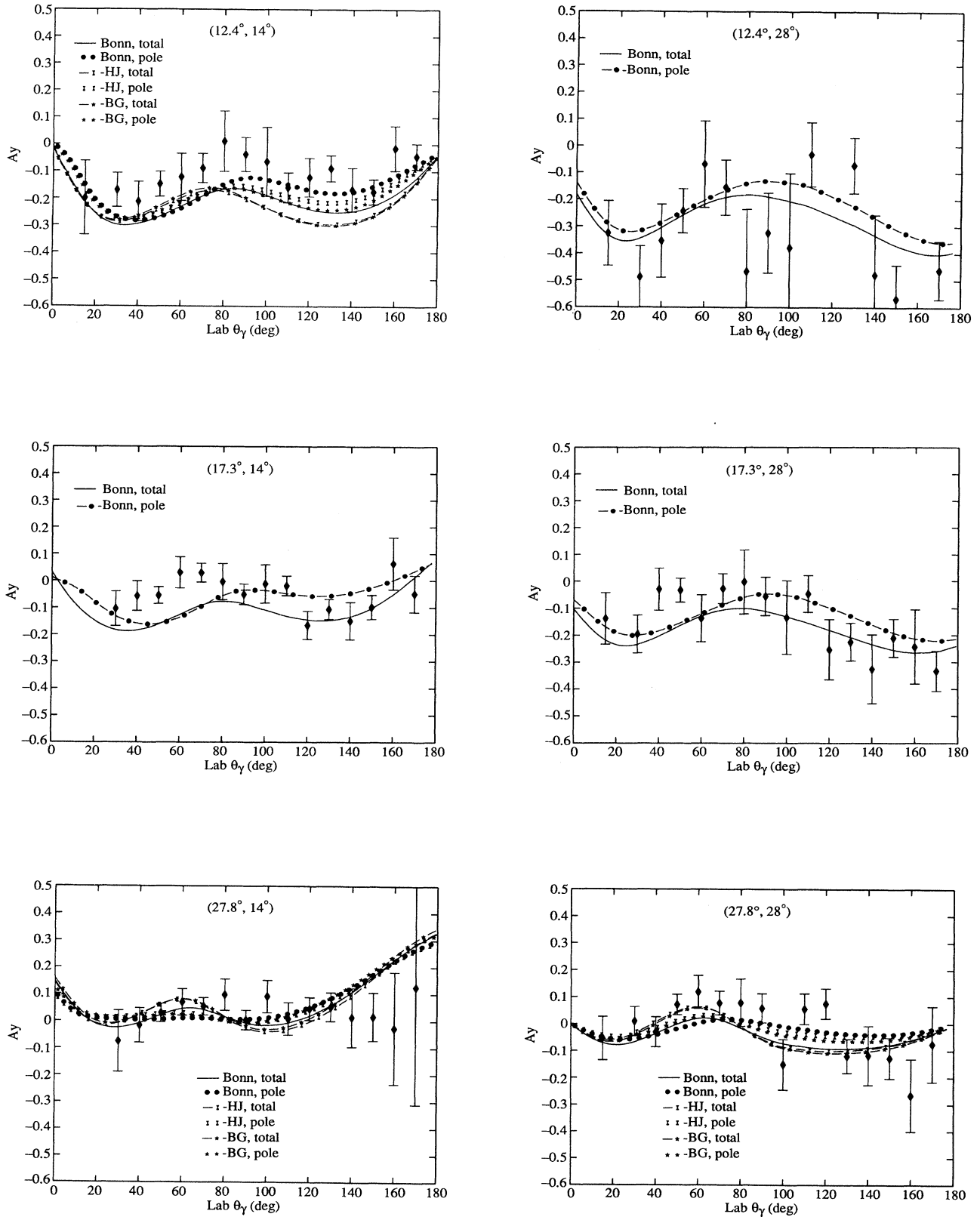


FIG. 12. The same as Fig. 11 with the contribution (pole) from the four-pole diagrams shown separately from the total, which includes the rescattering. The geometries shown are representative samples from Figs. 10 and 11. The Bonn potential is shown alone in three cases for ease in reading.

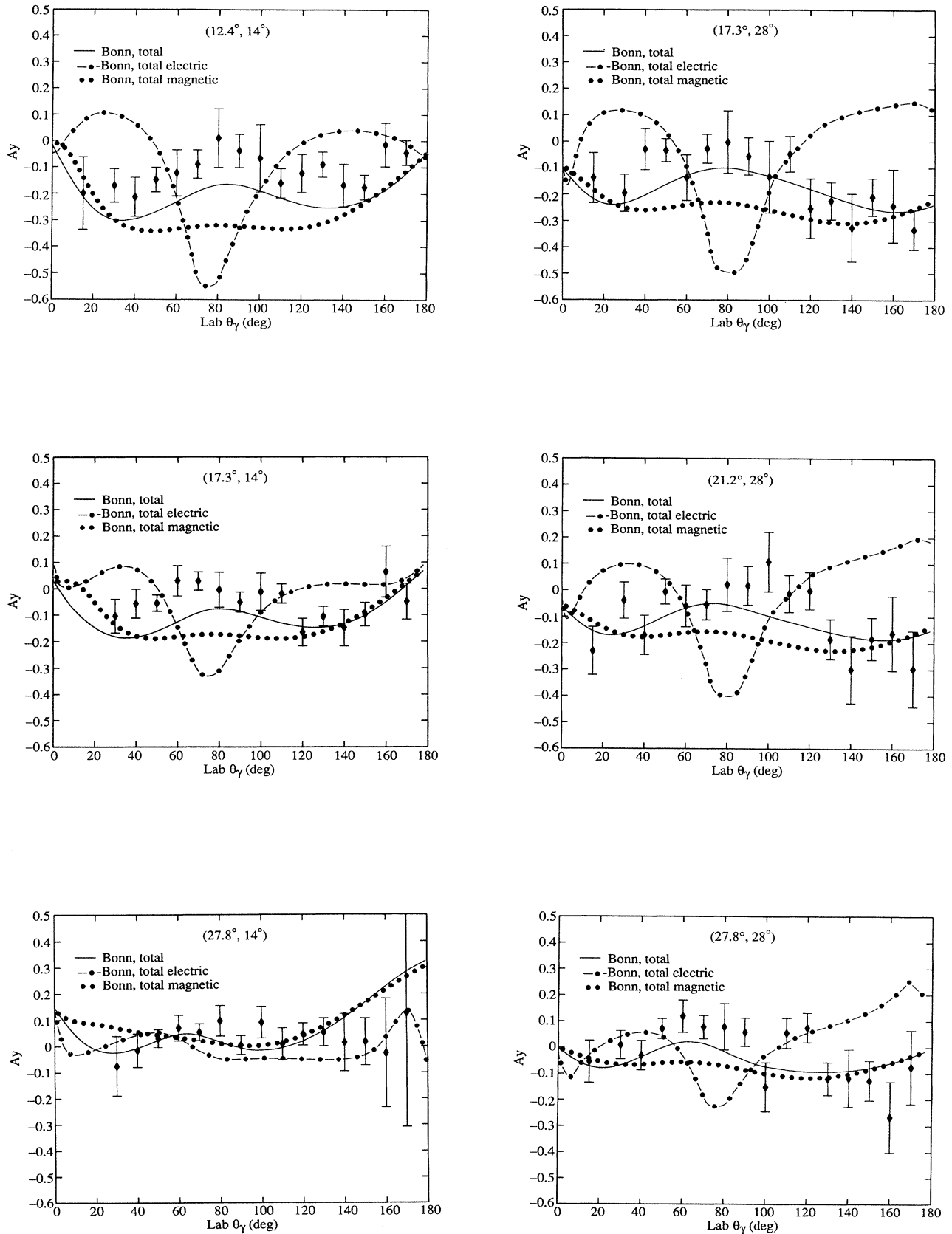


FIG. 13. The same as Fig. 11 with the electric and magnetic contributions to the total analyzing power separated (see text).

limit) situation of 90° , the on-shell and off-shell contributions to $NN\gamma$ converge. Figure 9 illustrates that the differential cross section and analyzing power, comparing the three potentials, are nearly equal as this elastic limit is approached. Since the results for the three potentials are so similar, only the Bonn potential is shown for the other parts of Fig. 9. The separation of the electric and magnetic parts shows that although the magnetic part is not negligible, the cross section and analyzing power are dominated by the electric contribution, and the angular distribution is consistent with an $E2$ behavior. This is in contrast to the domination of the magnetic terms in the more off-shell TRIUMF geometries.

III. CONCLUSIONS

A comparison of the present calculations to the TRIUMF data at 280 MeV gives different results from the calculation due to Fearing and collaborators [4]. In our calculation reasonable agreement with experiment for the Bonn potential is achieved without an arbitrary normalization of $\frac{2}{3}$ applied to the data. The contribution from rescattering depends on the kinematical situation. It tends to increase for small nucleon exit angles, which corresponds to larger photon momentum or larger off-shell contributions. The contribution from rescattering in the present calculations is up to approximately 20% in the differential cross section, but this is not enough to explain the differences in the two calculations. Another difference is that relativistic-spin corrections are treated in Ref. [4]. Since the effect on the calculations is not explicitly shown, it is not possible to analyze this difference.

The contribution to $pp\gamma$ from relativistic spin corrections [14–16] (RSC) has been left out of our calculations. We have shown that the magnetic contributions, for which the RSC are important, dominate the TRIUMF data. It would therefore be prudent to include the RSC before any final conclusions about agreement between the TRIUMF experiment and theory can be made. Since the rescattering cross sections which we have included increase the cross section by about 20%, these two effects could be of comparable size.

Our results are in better agreement with another calculation by Hermann and Nakayama [17], a recent paper, but this is not surprising since the code of Hermann and Nakayama has been compared with and brought into agreement with ours by a change in the phase-space calculation of their code.

The rescattering included in our work accounts for an increase of up to approximately 20% in the differential cross section and up to a factor of 2.5 in the analyzing

power. The fact that the rescattering contribution increases as the protons go more off shell emphasizes the importance of a consistent treatment of the rescattering term in looking for evidence of off-shell behavior of the nuclear T matrix.

One should keep in mind that since off-shell contributions from different potentials are not necessarily expected to be equal to each other nor to experiment, agreement with experiment need not imply a better bremsstrahlung calculation. Agreement with experiment would indicate that a potential extrapolates off the energy shell in the proper way. It could be that none of the many models for the NN interaction have the proper extrapolation. However, it appears that all the potentials we have presented here do extrapolate in a similar way.

For most cases, the Bonn results are closer to experiment than the other two potentials. This may be due to the fact that the Bonn potential is fitted to a modern data set. However, since the radial Bonn and the Bryan-Gersten potentials have similar short-range behavior, one is tempted to conclude that the weaker tensor force (stronger ρ to π meson contribution) for the Bonn potential may be favored by the $pp\gamma$ TRIUMF data. We have shown [1] a high degree of sensitivity to the tensor interaction in $pp\gamma$, where the magnetic terms dominate and spin degrees of freedom play an important role. The inclusion of the off-diagonal tensor-force contribution for $J \leq 4$ at 158 MeV ($30^\circ, 30^\circ$) reduced the forward differential cross section by 20% in our earlier work [1]. This is consistent with the fact that the Bonn potential gives larger $pp\gamma$ results. In order to make any meaningful conclusions, it is necessary to distinguish on-shell and off-shell tensor contributions in all partial waves, which is currently underway.

In order to examine the sensitivity of $NN\gamma$ to off-shell information, we have investigated¹⁸ other polarization asymmetries using a new on-shell approach. These measurements, which involve polarization of the beam and the target, are shown to have an even higher sensitivity to off-shell information than the measurements discussed here.

ACKNOWLEDGMENTS

The work was performed under the auspices of the U.S. Department of Energy at LLNL under Contract No. W-7405-ENG-48 and Grant No. SF-ENG-48. In addition, one of the authors (V.R.B.) wishes to thank Josef Speth and the IKP/KFA Juelich, West Germany, where part of this work was completed, for their generous support and hospitality.

[1] V. R. Brown, Phys. Rev. **177**, 1498 (1969); see also Phys. Lett. **25B**, 506 (1967).
 [2] R. A. Bryan and B. L. Scott, Phys. Rev. **177**, 1435 (1969).
 [3] T. Hamada and I. D. Johnston, Nucl. Phys. **34**, 382 (1962).
 [4] K. Michaelian *et al.*, Phys. Rev D **41**, 2689 (1990); see

also P. Kitching *et al.*, Nucl. Phys. A **463**, 87c (1987).
 [5] J. G. Rogers *et al.*, Phys. Rev. C **22**, 2512 (1980).
 [6] R. Machleidt, K. Holinde, and Ch. Elster, Phys. Rep. **149**, 1 (1987).
 [7] M. Lacombe *et al.*, Phys. Rev. C **21**, 861 (1980).

- [8] The radial Bonn potential used here is from Appendix F of Ref. [6].
- [9] R. A. Bryan and A. Gersten, *Phys. Rev. D* **6**, 341 (1972); **7**, 2802 (1973).
- [10] T. Hamada, Y. Nakamura, and R. Tamagaki, *Prog. Theor. Phys.* **33**, 769 (1965).
- [11] H. W. Fearing, *Phys. Rev. C* **22**, 1388 (1980).
- [12] The differential-cross-section and analyzing-power angular distributions shown in Figs. 3–13 were determined by about 30 calculated values on a θ_γ mesh with intervals of approximately 5° . A spline procedure was used to connect the calculated points with smooth curves.
- [13] We have checked that the polarized cross sections that determine the analyzing power also reproduce the unpolarized cross sections.
- [14] R. L. Workman and H. W. Fearing, *Phys. Rev. C* **34**, 780 (1986).
- [15] M. K. Liou and K. S. Cho, *Nucl. Phys.* **A160**, 417 (1971); M. K. Liou and M. I. Sobel, *Ann. Phys.* **72**, 323 (1972).
- [16] L. S. Celenza, M. K. Liou, M. I. Sobel, and B. F. Gibson, *Phys. Rev. C* **8**, 838 (1973).
- [17] V. Herrmann and K. Nakayama (unpublished).
- [18] V. R. Brown, P. L. Anthony, and J. Franklin (unpublished).